MECHANIKA TEORETYCZNA
I STOSOWANA
Journal of Theoretical
and Applied Mechanics
3, 31, 1993

IMPROVEMENT OF A ROBOT PERFORMANCE DUE TO ELIMINATION OF BOTH DYNAMIC INTERACTIONS AND JOINT LIMITS IN THE MANIPULATOR ARM

KAZIMIERZ NAZARCZUK

Institute of Aviation Engineering and Applied Mechanics
Warsaw University of Technology

The possibility of improvement of a robot capabilities due to the elimination of both dynamic interactions and joint limits in its arm has not been fully exploited till now. Two different dynamic schemes of such an arm driven directly have been presented. A manipulator 1:5 model revealing the complete dynamic interactions elimination due to the suitable mass distribution in terms of a proper driving motors arrangement has been shown. Basing on the presented dynamic analysis one can state that the designs being proposed ensure a considerable simplification of the robot control system as well as a great shortening of time taken in some motions.

1. Introduction

Improvement of a robot performance by means of versatility, dexterity, positioning accuracy, high speed motion and tracking precision, requires a permanent design study.

In recent years however, the possibility of introducing the direct drive systems into industrial robots has created a new perspective and new problems in manipulator design. In a direct drive manipulator arm high torque motors are directly coupled to each joint. This results in high mechanical stiffness, no backlash and low friction observed in the structure, but also implies significant interactions between the individual degrees of freedom (DOF), further intensified by the very high speed that the arm can reach, Asada et al. (1986). Synthesis of digital control systems which would enable us to compensate the above interactions in real time, is a very difficult and expensive problem, Vukobratovic et al. (1992).

Asada and Youcef-Tuomi (1984), have shown that dynamic interactions can be eliminated by the mass redistribution and modification of the arm structure. The design guidelines for this procedure, based on the concept of a decoupled and/or

configuration-invariant inertia matrix, have been formulated by Asada (1986) and Korendyasev et al. (1988).

For the decoupled and invariant inertia matrix, the arm with n DOFs can be treated as a system of n independent linear subsystems with constant parameters. As a result, the control system of the manipulator can be simplified and the control performance can be improved due to reduced dynamic complexity.

In this paper a new concept of the manipulator design is proposed and carefully studied. This design, due to application of the direct drive motors and a special transmission mechanism, ensure the elimination of the dynamic interactions as well as joint limits in the manipulator arm.

2. Influence of singularities and joint limits on the manipulator performance

Up till now all industrial robots have suffered from joint limits, which occur due to some constructional reasons and the common tendency to eliminate the singular configurations of manipulators.

The end-effector location (position and/or orientation) $\boldsymbol{x} \in R^m$ of a manipulator can be described by the vector of joint coordinates $\boldsymbol{q} \in R^n$ using the following nonlinear equations

$$\boldsymbol{x} = \boldsymbol{f}(\boldsymbol{q}) \tag{2.1}$$

By differentiating Eq (2.1) we obtain the linear relation between joint velocity $\dot{\boldsymbol{q}}$ and cartesian velocity $\dot{\boldsymbol{x}}$

$$\dot{\boldsymbol{x}} = \mathbf{J}(\boldsymbol{q})\dot{\boldsymbol{q}} \tag{2.2}$$

where $\mathbf{J}(\boldsymbol{q}) = \frac{\partial \boldsymbol{f}(\boldsymbol{q})}{\partial \boldsymbol{q}} \in R^{m \times n}$ is the jacobian matrix of a manipulator.

For the majority of manipulators $m = n = 6$ and $\mathbf{J}(\boldsymbol{q})$ is the 6×6 square matrix.

At regular configurations the jacobian matrix is invertible and we obtain

$$\dot{\boldsymbol{q}} = \mathbf{J}^{-1}(\boldsymbol{q})\dot{\boldsymbol{x}} \tag{2.3}$$

When the manipulator appears to be in a singular configuration, the jacobian matrix is non-invertible. Thus at a singular configuration the manipulator may lose one or more DOFs and can not reproduce the requested trajectories.

A scalar value w given by

$$w = \sqrt{\det \mathbf{J}\mathbf{J}^{\mathrm{T}}} \tag{2.4}$$

was introduced by Yoshikawa (1985) as a manipulability measure. When $m = n$, the manipulabity measure is simply given by

$$w = |\det \mathbf{J}| \tag{2.5}$$

At singular points $w = 0$.

In many algorithms the manipulability measure creates a criterion for the singularity avoidance. Example of such an algorithm is the singularity rubust (SR) inverse algorithm, introduced by Nakamura (1985), which facilitates the control of the manipulator in the vicinity of the singular configurations, but the manipulator performance at these points can not be improved by that algorithm.

The manipulator should not then come close to the singular configuration during its normal operation. In some manipulators singular configurations have been completely eliminated due to suitable means limiting the range of a particular DOF, the so-called joint limits. This restrictive safeguard considerably diminishes the manipulator applicability, what can be easily seen from Fig.1a, showing the workspace of a manipulator with two joints. The workspace in the case with no "joint limits" has a form of ring, the internal radius of which equals $r_{min} = |l_1 - l_2|$ and the external one equals $r_{max} = l_1 + l_2$, where l_1 and l_2 – lengths of the links 1 and 2, respectively. The singular configurations occur for $\Theta_2 = 0$ (points on the external circle) and for $\Theta_2 = \pi$ (points on the internal circle). At each point lying within this complete workspace two different configurations are permissible.

All the configurations for which $\Theta_2 \in <0, \pi>$ make up the so-called aspect A (Tsai et al., 1990), while the aspect B contains all the configurations for which $\Theta_2 \in <\pi, 2\pi>$.

The singular configurations are elements of both the aspects A and B, so the change of the aspect is possible only at singular configurations. When one introduces the limit in form of the inequality $0 \leq \Theta_2 \leq \pi$, valid e.g. for some SCARA type robots, configurations being the elements of aspect A are the only permissible ones.

The limitations of the motion range, usually introduced into the manipulator design, define the terminal positions, marked in Fig.1a by broken lines. In this case two regions corresponding to both aspects can be found. These regions hatched in Fig.1 in two different ways have also been denoted by A and B. Only at points lying on the common part of these regions (hatched in Fig.1) the proper configurations are possible. Each of these configurations enables different capabilities of the manipulator. In Fig.1b one can see for example the different ranges of speed reached at point P in the cases corresponding to both aspects, marked like in Fig.1a. The majority of conclusions which can be drawn from the example shown in Fig.1 concerns any manipulator forming an open kinematic chain. There is only a different number of permissible configurations, which equals the number of possible solutions to the inverse kinematical problem, for each end-effector position and orientation, respectively.

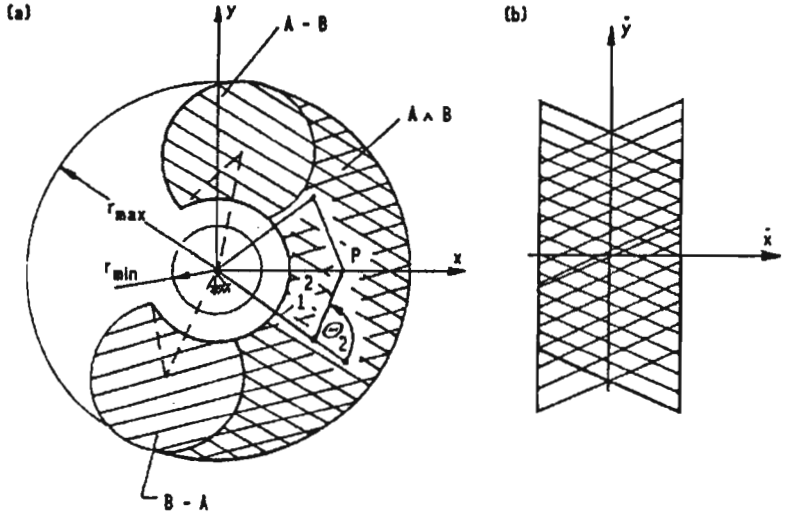

Fig. 1.

In the case of manipulator design with six revolute joints ($6R$) the number of permissible configurations equals 16, but when the axes of these joints intersect at one point, this number decreases to 8 (Raghavan et al., 1990). The latter case concerns many kinds of industrial robots supplied with a spherical wrist, in which two different wrist configurations and four different arm configurations are permissible. The kinematical analysis of a manipulator supplied with a spherical wrist can be decomposed into two separate problems, one concerning the arm, i.e. the so-called "regional structure" and the other dealing with the wrist, i.e. the "orientation structure".

Many different means for determination of the workspace of the robot arm despite its structure, together with the methods of the so-called "boundary surfaces" (jacobian surfaces) dividing the workspace into regions corresponding to different aspects have been developed till now.

The influence of both the arm geometrical structure and the joint limits on these regions shape and size has also been carefully studied.

Conclusions drawn by Kohli and Migh-Shu (1987), Parenti, Castelli and Innocenti (1988), concerned mainly the conditions under which the large volume and the suitable shape of the workspace occur. In the latest works much more attention has been paid to the problem of conditions under which the size of a region with a high number of permissible configurations can be extended (cf Lenarcic et al., 1992; Tsai and Chiou, 1990). Lenarcic et al. (1992) has introduced the term "kinematic flexibility" which denote the number of permissible manipulator configurations corresponding to the end-effector position and orientation.

The kinematic flexibility has been applied as a criterion for the manipulability assessment.

The best way to increase the kinematic flexibility is the complete elimination of the joint limits which enables also the changes in configuration. On the other hand this results in enlarging such jacobian areas within the workspace in which suitable computation algorithms have to be applied in the control system, e.g. the SR-inverse algorithm.

Basing on the considerations given by Marroidis and Roth (1992), Raghavan and Roth (1990), Rastegar and Deravi (1987), one can arrive at the conclusion that the $6R$ manipulator arm with a simple inverse kinematic analysis, supplied with a spherical wrist and revealing no joint limits, which ensures 8 permissible configurations at each point lying within the workspace can be designed. Many different manipulator designs allowing for the revolute motion in the wrist joints of the range considerably exceeding 360° have emerged lately. To the Author's best knowledge in the present literature one can not find the manipulator arm design without limits since it is very difficult to create a compact, light and stiff design of such an arm.

It is reasonable to conclude that the remarkable advantages of such a design would be noticeable only if both the joint limits and the dynamic interactions were eliminated.

3. Influence of dynamic interactions on the manipulator properties

These interactions can be represented as certain components of the generalized forces acting upon the manipulator arm, what can be written as

$$\mathbf{A}(q)\ddot{q} + B(q,\dot{q}) + G(q) = T \tag{3.1}$$

where

- q – vector of joint displacements
- T – vector of joint torques
- $G(q)$ – vector of gravitational forces
- $\mathbf{A}(q) \in R^{n\times n}$ – inertia matrix
- $B(q,\dot{q}) \in R^n$ – vector of the Coriolis and centrifugal forces.

Each line of Eq (3.1) has the following form

$$\sum_{j=1}^{n} A_{ij}\ddot{q}_i + \sum_{j=1}^{n}\sum_{k=1}^{n} B_{ijk}\dot{q}_j\dot{q}_k + G_i = T_i \qquad (i = 1,2,...,n) \tag{3.2}$$

where

$$B_{ijk} = \frac{1}{2}\left(\frac{\delta A_{ij}}{\delta q_k} + \frac{\delta A_{ik}}{\delta q_i} - \frac{\delta A_{jk}}{\delta q_i}\right) \tag{3.3}$$

are the Christoffel's symbols.

The computation of the vector T, in general, requires the use of efficient algorithms for the inverse dynamic problem and high-efficiency microcomputer systems. The problem is somewhat simplified in the case of geared manipulators, since the effects of time-varying inertia are reduced by a factor r_i^2, where r_i is the gear ratio, while the interaction torques and the nonlinear torques are similarly reduced by a factor r_i. Thus, the simplified Eq (3.2) has actually of the form (Asada and Slotine, 1986)

$$(A_{mi} + A_{ai} r_i^{-2})\ddot{q}_i + (T_{ci} + T_{ni}) r_i^{-1} = T_i \tag{3.4}$$

where

- A_{mi} – the invariant inertia of the motor including the gear
- A_{ai} – the arm inertia reflected to the joint axis
- T_{ci} – the interactive inertia torque (i.e. the terms in $A_{ij}\ddot{q}_j$ for $i \neq j$)
- T_{ni} – nonlinear (centrifugal, Coriolis and gravity) torque reduced to the joint axis.

A simplified dynamic model of a manipulator in terms of Eq (3.4) is used in typical control systems for industrial robots. In this case each joint is controlled by its own independent position servo.

For a typical point to point (PTP) control, dynamic interactions may play an insignificant role. For continuous paths (CP) control, however, dynamic interactions have an essential influence on the tracking precision (Gosiewski, 1992)

In the case of direct drive robots, the gear ratio $r_i = 1$, what results in the fact that Eq (3.2) can not be applied any more, even to a simplified dynamic analysis.

4. Design study of the elimination of dynamic interactions and joint limits in the manipulator arm

From Eq (3.1) ÷ (3.3) it follows that the dynamic model of manipulator arm can be considerably simplified when designed in a form ensuring both static balance (i.e. $G(q) = 0$) and diagonality of the inertia matrix irrespective of the configuration. In such a case the terms of matrix A should fulfil the following conditions

$$\begin{aligned} A_{ij} &= \text{const} \quad && \text{for} \quad i = j \\ A_{ij} &= 0 && \text{for} \quad i \neq j \end{aligned} \tag{4.1}$$

Eqs (3.2) can then be rewritten as

$$A_{ii}\ddot{q}_i = T_i \qquad (i = 1, 2, ..., n) \tag{4.2}$$

According to Korendyasev et al. (1988), the following two conditions should be satisfied to make the simplified dynamic model of the manipulator arm: applicable

1. independence of the kinetic energy from the configuration;

2. the proper selection of the set of joint displacements (which are usually the actuator coordinates), such that the formula for the kinetic energy may be reduced to a canonical form (i.e. representation by a sum of terms depending only on squares of joint velocities).

Basing on the sugestions given by Asada (1986) and Korendyasev et al. (1988), the Author proposes below two different designs of a manipulator arm with three revolute DOFs, for which it is possible to eliminate both the dynamic reactions and the joint limits.

The first one, the scheme of which is shown in Fig.2a, is a slight modification of the PUMA robot. The arm drive consists of three direct drive motors. It should be mentioned that links 1 and 2 are really directly driven by motors M_1 and M_2, while link 3 is driven remotely by motor M_3 through a gear the ratio of which equals 1. Motors M_2 and M_3 are fixed on link 1 in a collinear way. New direct drive motor designs enable such a collinear mounting of even several motors due to their shape in the form of a ring.

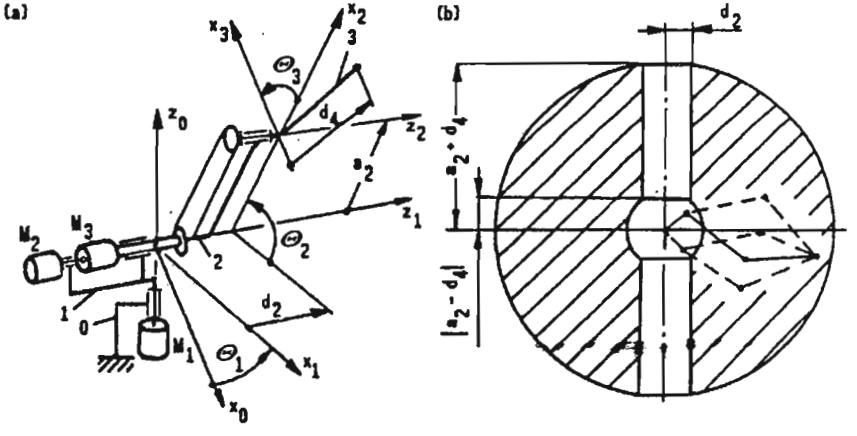

Fig. 2.

Fig.2a shows also the local coordinate systems fixed to links $0 \div 3$ according to the Denavit-Hartenberg convention. All the ith local systems (orthogonal and dextral) are represented in the figure by axes x_i and z_i.

The manipulator design enables the revolute motions in every joint without any limits.

For the kinetic energy to be independent of the configuration the arm design should meet the following conditions

A. z_2 axis overlaps the principal axis of link 3, while the moments of inertia about the remaining principal axes are equal. The tensor of inertia of link 3 has then the following form

$$\mathbf{I}^{(3)} = \begin{bmatrix} J_{11}^{(3)} & 0 & 0 \\ 0 & J_{22}^{(3)} & 0 \\ 0 & 0 & J_{33}^{(3)} \end{bmatrix} \tag{4.3}$$

while $J_{11}^{(3)} = J_{22}^{(3)}$.

It is assumed that the center of mass of link 3 is located at the local coordinate system $x_2y_2z_2$ origin.

B. The location of link 2 mass center relative to the $x_2y_2z_2$ coordinate system is defined in terms of the vector given below

$$\mathbf{r}_{c2} = [x_{c2}, 0, 0]^{\mathrm{T}} \tag{4.4}$$

The inertia tensor of link 2 has the form

$$\mathbf{I}^{(2)} = \begin{bmatrix} J_{11}^{(2)} & 0 & 0 \\ 0 & J_{22}^{(2)} & 0 \\ 0 & 0 & J_{33}^{(2)} \end{bmatrix} \tag{4.5}$$

where

$J_{33}^{(2)}$ – moment of inertia of link 2 about the principal axis parallel to z_1

$J_{11}^{(2)}$ – moment of inertia about the x_2 axis

$J_{22}^{(2)}$ – moment of inertia about the third principal axis satisfying the following condition

$$J_{11}^{(2)} = J_{22}^{(2)} + (x_{c2} - a_2)^2 m_2 + a_2^2 m_3 \tag{4.6}$$

Condition B establishes that link 2 supplied with the mass of link 3 can be treated as a rigid body, principal axis of which overlaps the z_1 axis, while the moments of inertia about the remaining principal axes are equal.

If one assumes the following joint coordinates

$$q_1 = \Theta_1 \qquad q_2 = \Theta_2 \qquad q_3 = \Theta_2 + \Theta_3 \tag{4.7}$$

the dynamic model of the arm shown in Fig.2a is then described by three independent equations in the form of Eq (4.2) and

$$A_{11} = J_{33}^{(1)} + r_{c1}^2 m_1 + d_2^2(m_2 + m_3) + J_{11}^{(2)}$$

$$A_{22} = J_{33}^{(2)} + a_2^2 m_3 \tag{4.8}$$

$$A_{33} = J_{33}^{(3)}$$

where r_{c1} – the distance between the link 1 center of mass and the z_0 axis.

Fulfilling the condition B is rather difficult, especially making Eq (4.6) valid, and results in a considerable increase in the link 2 inertia.

The arm design presented above will probably find no application despite of the suitable workspace shape shown in Fig.2b.

The second design, scheme of which is shown in Fig.3a, seems to be a much more promising one. The first two DOFs are the same like in the SCARA robot, but link 2 is driven remotely by M_2 motor through a transmision mechanism with the ratio equal to 1. Motors M_2 and M_1 (driving link 1) are mounted in a collinear way on the fixed frame. The third DOF (about the horizontal axis) is driven by M_3 motor fixed on link 2.

In this case when the kinetic energy of an arm is independent of the configuration, both the condition A is fulfilled and the center of mass of links 2 and 3 is located on z_1 axis. It is worth mentioning that there is no need for introducing the special counterbalances to ensure the proper distribution of the masses of links 2 and 3. The M_3 motor together with the motors driving the wrist should be used for this.

Assuming the following joint coordinates

$$q_1 = \Theta_1 \qquad q_2 = \Theta_1 + \Theta_2 \qquad q_3 = \Theta_3 \tag{4.9}$$

one obtains the equation of motion in the form of Eq (4.2), while

$$A_{11} = J_{33}^{(1)} + r_{c1}^2 m_1 + a_1^2(m_2 + m_3)$$

$$A_{22} = J_{33}^{(2)} + J_{11}^{(3)} + r_{c2}^2 m_2 + r_{c3}^2 m_3 \tag{4.10}$$

$$A_{33} = J_{33}^{(3)}$$

where r_{ci} denotes the distance between the ith link center of mass and the corresponding axis of revolution.

A cross-section through the workspace is shown in Fig.3b, while Fig.3c presents the four permissible arm configurations with the end-effector position remaining unchanged. The workspace has smaller volume but its shape, in turn, ensures

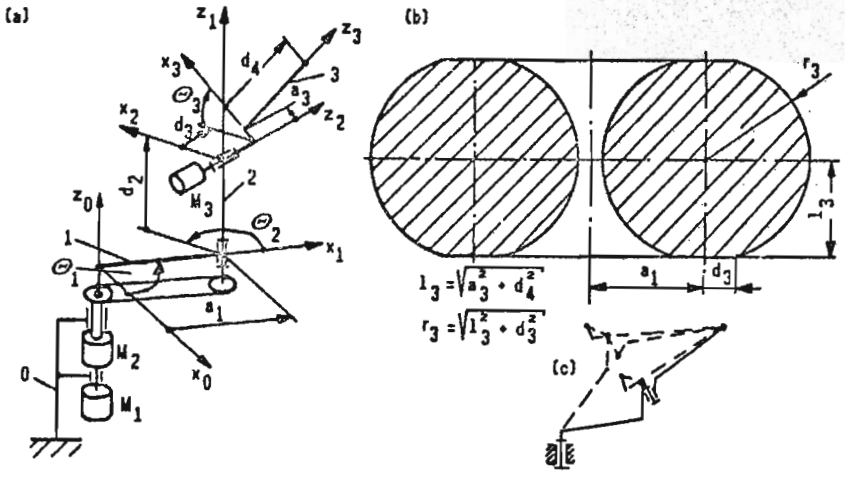

Fig. 3.

the simpler movement to another aspect than in the case of the PUMA robot. Bidziński et al. (1992), presented the kinematic analysis of the robot with the same kinematic scheme, but also with the joint limits which restricted the arm workspace to the region where only 1 aspect is permissible (1 configuration at every point).

Basing on the considerations given above the primary structural assumptions for the 6 DOFs manipulator arm of the scheme shown in Fig.3a, supplied with a spherical wrist, have been formulated. According to these assumptions the 1:5 model of the manipulator has been built (see Fig.4).

Direct drive motors have been applied to the arm drive, while the wrist is driven through gears.

The first DOF of the arm together with the third DOF of the wrist exhibit the motion range without any limits. In the two other joints the ranges of motion are limited to $\pm 4\pi$ due to the electrical wires twisting.

The crucial element of the design is the mechanism realizing the link 2 remote drive with no motion limits and wires twisting. Design details of this mechanism will be given after completing the experiments.

A unique shape of link 3, shown in Fig.4, enables the condition A to be satisfied without any obstacles, by means of the proper arrangement of the wrist driving motors, treated as counterbalances.

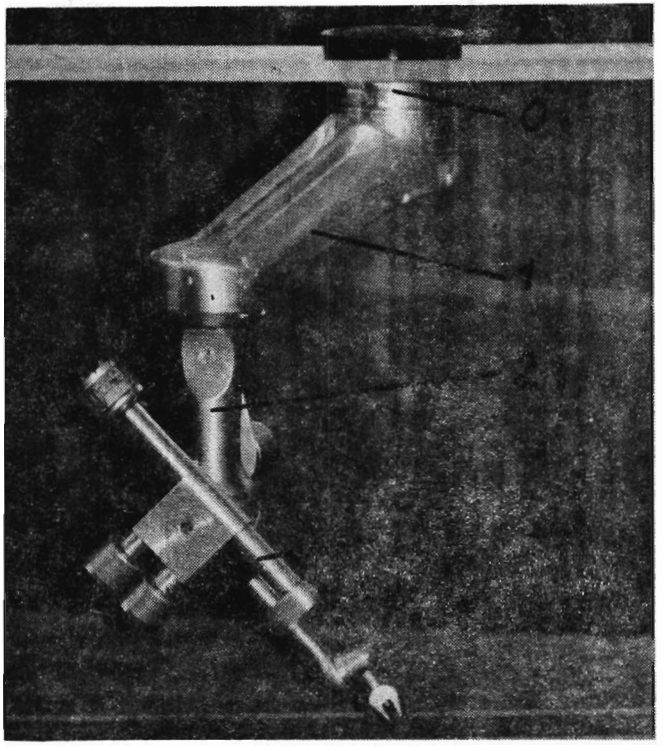

Fig. 4.

5. Some remarks concerning the time-optimal control

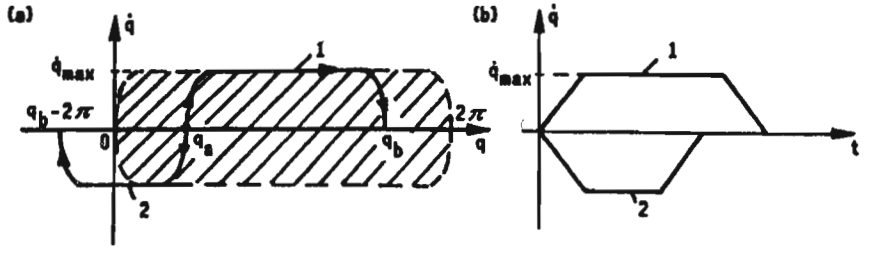

Fig. 5.

The advantages of the presented simplified model with respect to the control system have been shown in the first section of this paper. It is worth mentioning

that the arm joint limits elimination results also in considerable profits, primarily due to the fact that the change in the coordinate q can be made in two different ways. This is of essential importance for the time-optimal control over the joint velocity profile shown in Fig.5b, since it enables to find the shorter time trajectory on the phase-plane (see Fig.5). Coordinates q_b and $q_b - 2\pi$ correspond to the same joint configuration. The time required for passing from q_a to q_b is much shorter along the trajectory 2 then along the trajectory 1. The second considerable advantage consists in the fact that there is no such region in the workspace, within which the manipulator reveals poorer performance capabilities due to the limited number of aspects or the necessity of braking in front of the joint limit. The region of the phase-plane hatched in Fig.5 a consists of all the permissible states of the considered DOF in the case when a zero-dimensional limit occurs in the joint. After elimination of this limit, the area of permissible states is restricted only by the maximum speed condition

$$|\dot{q}| \leq \dot{q}_{max}$$

It can be easily shown that under the time-optimal control in the joint space the maximum time interval required for any state change of the decoupled dynamic manipulator with zero-dimensional joint limits is twice as long as after the elimination of these limits. The aforementioned conclusion concerns of course any case in which the trajectory profile from the initial to the final state is of secondary importance.

The elimination of joint limits and the easy way of the aspect changing enable also a considerable shortening of the time taken in motion along a specified path. This can be proved on the basis of the dynamic analysis carried out in the cartesian space. By differentiating Eq (2.2) with respect to time one obtains the formula for the acceleration vector $\ddot{x} \in R^m$

$$\ddot{x} = \mathbf{J}(q)\ddot{q} + \dot{\mathbf{J}}(q,\dot{q})\dot{q} \tag{5.1}$$

where $\dot{\mathbf{J}}(q,\dot{q}) \in R^{m \times n}$.

Each entry $\dot{J}_{ij}$ of the matrix $\dot{\mathbf{J}}(q,\dot{q})$ has the following form (Chevallereau and Mohammed, 1992)

$$\dot{J}_{ij} = \sum_{k=1}^{n} \frac{\delta J_{ij}}{\delta q_n}\dot{q}_k \qquad \begin{matrix}(i = 1,2,...,m)\\(j = 1,2,...,n)\end{matrix} \tag{5.2}$$

The generalized acceleration vector $\ddot{q}$ can be determined using Eq (3.1) since the matrix $\mathbf{A}(q)$ is invertible; we can write then

$$\ddot{q} = \mathbf{A}_q^{-1}[T - B(q,\dot{q} - G(q)] \tag{5.3}$$

In the case when all the dynamic interactions in the manipulator arm are eliminated the formula given above is simplified considerably

$$\ddot{q} = \mathbf{A}^{-1}T \tag{5.4}$$

where $q \in R^3$, $T \in R^3$, $\mathbf{A} \in R^{3\times3}$.

Substituting Eq (5.4) into Eq (5.1) and applying Eq (5.2) after some transformations one obtains

$$\ddot{x} = \mathbf{J}(q)\mathbf{A}^{-1}T + v^2C(q, e_v) \tag{5.5}$$

where

- $v \in R$ – end-effector cartesian speed absolute value
- $e_v \in R^3$ – unit vector (e_v lies on the tangent to the path at the point under consideration)
- $C(q, e_v) \in R^3$ – vector defining the component of acceleration $\ddot{x}$ depends on the initial conditions only, defined by vectors q and e_v for $v = 1$.

The formula in the form of Eq (5.5) obtained by substituting Eq (5.3) into Eq (5.1) was used by Thomas et al. (1985), for dynamic analysis of the manipulator. A similar formula in terms of the coordinates fixed to the specified path was applied by Dubovski and Shiller (1984) to the time-optimal control problem solution. They showed also that under specified limits the driving moments have the form

$$T_{i\min} \leq T_i \leq T_{i\max} \tag{5.6}$$

the range of reachable accelerations tangential to the path contracts as the absolute value of the velocity increases. For a high enough value of v ($v = v_{\max}$) this range reduces to a point and motion along the specified path can be performed only at a speed lower than $v_{\max}$. The Author proves below that this is not a general formula, i.e. it does not concern all the possible cases.

Focusing only on Eq (5.5) we can write the formula for the vector $\ddot{x}$ in a form of tangential $\ddot{x}_v$ and normal $\ddot{x}_n$ components, respectively

$$\ddot{x} = \ddot{x}_v + \ddot{x}_n \tag{5.7}$$

where

$$\ddot{x}_v = \dot{v}e_v \tag{5.8}$$

$$\ddot{x}_n = kv^2e_n \tag{5.9}$$

k denotes the first slope of the path, e_n stands for the unit normal vector to the path.

For $v = 0$

$$\ddot{x} = \dot{v}e_v = \mathbf{J}(q)\mathbf{A}^{-1}T \tag{5.10}$$

When the limits of driving moments are symmetrical, i.e.

$$T_{i\min} = -T_{i\max} = T_m \tag{5.11}$$

then the set of permissible vectors $\ddot{x}$ at $v = 0$ creates the region in a form of a parallelepiped, center of which is located at the origin of the coordinate system. The extreme values of the tangential acceleration are determined by the points through which the faces of this parallelepiped are punched by the line overlapping the e_v vector.

In the case under consideration the symmetry condition results in $\dot{v}_{\min} = -\dot{v}_{\max}$.

For $v \neq 0$, basing on Eqs (5.5), (5.7) and (5.9) we can write

$$\dot{v}e_v = \mathbf{J}(q)\mathbf{A}^{-1}\boldsymbol{T} + v^2[\boldsymbol{C}(q, e_v) - ke_n] \tag{5.12}$$

In this case the area of permissible accelerations is translated with regard to the origin by vector $v^2\boldsymbol{D}$, where

$$\boldsymbol{D} = \boldsymbol{C}(q, e_n) - ke_n \tag{5.13}$$

The range of the permissible tangential accelerations usually decreases with the velocity increase (see Fig.6). When $\boldsymbol{D} = \mathbf{0}$, the extreme values $\dot{v}_{\min}$ and $\dot{v}_{\max}$ do not depend on v and equal the ones for $v = 0$. If $\boldsymbol{D} \neq \mathbf{0}$ but is collinear to the vector e_v the width of the permissible tangential accelerations range, equal to $v_{\max} - v_{\min}$, does not depend on v.

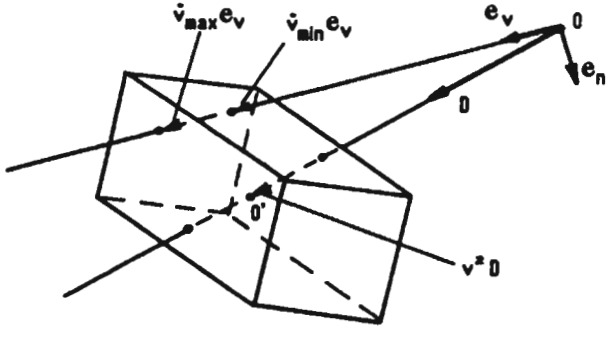

Fig. 6.

In such cases the value of the maximum speed is determined by other factors, especially the driving motors characteristics, $T_i(q_i)$, not considered in this paper.

The results of the above considerations should be taken into account when programming the robot task. It is worth mentioning that the form of the vector $\boldsymbol{C}(q, e_v)$ depends on the configuration which, in turn, is determined at a specified workspace point by the aspect. For the arm with the joint limits being eliminated four different aspects are permissible, so one should choose the most suitable one for the specified task.

6. Conclusions

The manipulator arm design, described above, in which the dynamic interactions together with the joint limits are eliminated may considerably improve the properties of electrical direct drive robots.

Profits form such a design consist in substantial simplification of the control system, extension of the workspace, kinematic flexibility increase and considerable shortening of the task realization time. The latter concerns mainly extent (parallel) motions performed under the PTP control.

In the case of the motion performed along a specified path the choice of the proper configuration may also ensure reaching a higher value of speed.

Looking at the model shown in Fig.4, with the arm, the kinematic scheme of which is presented in Fig.3, it may be proved that it is possible to describe an efficient manipulator design exhibiting the complete dynamic interactions elimination due to the suitable mass distribution in terms of a proper arrangement driving motors.

References

1. ASADA H., 1986, *The Kinematic Design and Mass Redistribution of Manipulators Arms for Decoupled and Invariant Inertia,* Proceedings of 6th CISM-IFToMM Symposium on Theory and Practice of Robots and Manipulators (Romansy 86) Cracow Poland, Ed. Hermes 1988, 221-245

2. ASADA H., YOUCEF- UOMI K., 1984, *Analysis and Design of a Direct-Drive Arm with a Five-Bar-Link Parallel Drive Mechanisms,* Trans of the ASME J. of Dynamic Systems, Measurements and Control, 106, 225-230

3. ASADA H., SLOTINE J.J.E., 1986, *Robots analysis and Control,* John Wiley and Sons, New York

4. BIDZIŃSKI J., MIANOWSKI K., NAZARCZUK K., SŁOMKOWSKI T., 1992, *A manipulator with an arm of serial-paralel structure,* Archiwum Budowy Maszyn, XXXIX, 1-2, 65-78

5. CHEVALLEREAU C., AIT MOHOMED A., 1992, *Dynamic Control of redundant robots in the cartesian space optimization by gradient method,* 81-86

6. DUBOVSKI S., SHILLER Z., 1984, *Optimal dynamic trajectories for robotic manipulators,* Preprints of 5-th CISM-IFToMM, Symp.on Theory and Practice of Robots and Manipulators, Udine-Italy, 96-104

7. GOSIEWSKI A., 1992, *Dynamicc Interactions in Robot Manipulators,* Robotic Research and Applications, Warszawa

8. KOHLI D. MIGH-SHU HSU, 1987, *The jacobian analysis of workspaces of mechanical manipulators,* Mech.Mach.Theory, 22, 3, 265-275

9. KORENDYASEV A.I., SALAMANDRA B.L., TYVES L.I., 1988, *Mechanics of Robots with Dynamically Decoupled Motions,* Proceedings of 7th CISM-IFToMM Symposium on Theory and Practiceof Robots and Manipulators, Romansy 86, Udine, Italy, Ed. Hermes 1990 448-455

10. LENARCIC J., STANIC U., OBLAK P., 1992, *Study of kinematic flexibility of standard welding robots,* Proc. of the 23rd Int.Symp. on Industral Robots, Barcelona, Spain, 277-282

11. MAVROIDIS C., ROTH B., 1992, *New manipulators with simple inverse kinematics,* Proc.of the 9-th CISM-IFToMM Symposium on Theory and Practice of Robots and Manipulators, Udine, Italy, (to appear)

12. NAKAMURA Y., 1985, *Ph.D.Dissertation,* Kyoto University

13. PARENTI C.V., INNOCENTI C., 1988, *Spatial Open Kinematic Chains, Singularities, Regions and Subregions,* Proc. of the 7th CISM-IFToMM Symp. on Theory and Practice of Robots Manipulators, Udine, Italy, Ed. Hermes 1990, 400-407

14. RAGHAVAN M., ROTH B., 1990, *A general Solution for the inverse kinematics of all series chains,* Proceedigs of the 8th CISM-OFToMM Symposium an Robots and Manipulators (Romansy-90) Cracow, Poland

15. RASTEGAR J., DERAVI P., 1987, *The effect of joint motion constrains on the workspace and number of configurations of manipulators,* Mech.Mach.Theory, 22, 5, 401-409

16. THOMAS M., YOUAN-CHOU H.C., TESAR D., 1985, *Optimal Actuator Sizing for Dynamic Criteria,* Journal of Mechanisms, Transmissions, and Automation in Design, 107, 163-164

17. TSAI M.J., CHIOU Y.H., 1990, *Manipulability of manipulators,* Mech. Mach. Theory, 25, 5, 575-585

18. VUKOBRATOVIC M., FILARETOV V., 1992, *Static balancing and dynamic decoupling of the motion robots,* Proc. of the 23 ISIR, Barcelona, Spain, 207-212

19. YOSHIKAWA T., 1985, *Analysis and Control of Robot Manipulator with Redundancy,* Proc.1st Int.Symp.Robotics Resarch, MIT Press. Cambridge, MA, 735-747

Poprawa własności robota poprzez jednoczesne wyeliminowanie interakcji dynamicznych oraz ograniczeń ruchu w przegubach jego ramienia

Streszczenie

W pracy zwrócono uwagę na niewykorzystaną dotychczas w pelni możliwość poprawienia własności robota poprzez jednoczesne wyeliminowanie interakcji dynamicznych oraz ograniczeń zakresów ruchów w przegubach jego ramienia. Zaproponowano dwa schematy kinematyczne takich ramion z elektrycznym napędem bezpośrednim. Przedstawiono model manipulatora wykonany w skali 1:5, w którym rozkład mas zapewniający eliminację interakcji dynamicznych ramienia uzyskuje się dzięki odpowiedniemu rozmieszczeniu silników napędowych. Z przeprowadzonej analizy dynamicznej wynika, że proponowane rozwiązania mogą zapewnić nie tylko istotne uproszczenie sterowania robotem, ale również znaczne skrócenie czasu niektórych ruchów.

Manuscript received April 5, 1993; accepted for print May 5, 1993